

A novel mooring tether for peak load mitigation: Initial performance and service simulation testing

Philipp R. Thies*, Lars Johanning

*CEMPS - College of Engineering, Mathematics and Physical Science
Renewable energy research group, University of Exeter
Penryn Campus, Treliever Rd, Penryn, TR10 9EZ, UK*

Paul McEvoy

*Technology from Ideas Ltd
Unit 3b, Cleaboy Business Park,
Old Kilmeaden Road
Waterford, Ireland*

Abstract

One of the main engineering challenges for floating marine renewable energy devices is the design of reliable, yet cost-effective mooring solutions for the harsh and dynamic marine environment. The mooring system must be able to withstand the ultimate limit state during storm conditions as well as the fatigue limit state due to the highly cyclic wave induced motions.

This paper presents the performance and service simulation testing of a novel mooring tether that combines the material properties of elastomeric and thermoplastic elements. This allows to 'tailor' the load-extension curve to exhibit a low stiffness response for the expected normal, operating, load conditions and a high stiffness response for the envisaged extreme, storm, conditions. The experimental results demonstrate the working principle of

*corresponding author, Tel.: +44 (0)1326 255849, Fax: +44 (0)1326 254243
Email addresses: P.R.Thies@exeter.ac.uk (Philipp R. Thies*),
paul.mcevoy@technologyfromideas.com (Paul McEvoy)

the mooring element and show good agreement between the theoretical load extension curve and the conducted performance tests with a distinct hysteresis effect caused by the thermoplastic element. The hysteresis is dependant on the applied pre-tension and load cycle amplitude of the element and to a lesser extent on the cycle frequency. The relaxation of the elastomeric element is quantified, giving insight into the expected long-term performance of the tether. The demonstrated working principle and the possibility to tailor the mooring response allows engineers to load- and cost-optimize the mooring system of floating marine energy converters.

Keywords: elastomeric mooring, component testing, offshore renewable energy, peak loads, reliability

1	Contents	
2	1 Introduction	4
3	1.1 Cost reduction potential for mooring systems	4
4	1.2 Brief review on use of rubber moorings	6
5	1.3 Scope and structure	7
6	2 Experimental set-up and procedures	8
7	3 Results	11
8	3.1 Performance tests	11
9	3.2 Amplitude and frequency hysteresis tests	13
10	3.3 Service simulation tests	14
11	3.3.1 Extreme tests	14
12	3.3.2 Fatigue tests	15
13	3.4 Creep Analysis	16
14	4 Discussion and Conclusion	17
15	References	20
16	List of Figures	24

17 **1. Introduction**

18 The development of wave and tidal energy holds the potential to alle-
19 viate issues of energy security, reduce carbon emissions and to build a new
20 industry. The progress so far has been confined to the installation of pro-
21 totypes and small-scale demonstration projects. However, recent activities
22 in the UK where the Crown Estate has leased marine energy sites for large
23 commercial-scale developments with a total capacity of 1.6GW are very
24 promising. The 11 projects in the Pentland Firth and Orkney waters are
25 expected to be installed during 2014-2020. Floating wave energy applica-
26 tions are planned with an installed capacity of 400MW [1]. Another area of
27 application that is increasingly considered is the mooring of floating offshore
28 wind installations [2, 3].

29 *1.1. Cost reduction potential for mooring systems*

30 One of the most critical components for all floating offshore devices is
31 the mooring system. The requirements and design issues are discussed in
32 [4-6]. Some of the key points which need to be accommodated are:

- 33 • Survival in extreme load conditions
- 34 • Allowing dynamic motions under operational conditions for power con-
35 version
- 36 • Long-term reliability
- 37 • Cost-effectiveness

38 The capital cost of present mooring systems is estimated to incur about
39 10% of the capital cost of a typical marine energy converter installation [7].
40 This cost estimate dates back to 2004 and may be overly optimistic for more

41 exposed sites with water depth larger than 50m. As a consequence, moor-
42 ing floating structures in exposed sites is expensive and needs to drop in
43 costs for devices to become viable. The mooring systems are typically being
44 adapted from oil and gas applications and carry high safety factors, while
45 they are not being optimally designed to accommodate the requirements for
46 wave energy devices. In particular for oil and gas installations peak loads are
47 of concern, as the mooring must be able to withstand the highest loads ex-
48 pected in storm conditions, which typically lie an order of magnitude above
49 the operational load conditions. This leads to an asymmetrical situation for
50 the case of marine energy converters where the mooring system carries the
51 capital expenditure for extreme conditions, while the potential for generated
52 income is constrained through operating conditions.

53 The mooring cost estimated by Johanning et al. [8] identifies mooring
54 lines and chains as the main cost factors with up to 70% of the overall
55 mooring system cost. The specific cost of mooring lines/chain is approxi-
56 mately linear to the required minimum breaking load (MBL). As such, peak
57 loads have a direct impact on the mooring cost. Or, to put it optimistically,
58 the mitigation of peak loads are of immediate benefit for the cost-efficiency
59 of the mooring system.

60

61 The mitigation of peak loads without incurring excessive MBL require-
62 ments of conventional mooring ropes can be achieved with innovative mooring
63 designs. One such technology has been developed by Techology from Ideas
64 (TfI), proposing a soft elastomeric, rubber element to provide the required
65 compliance during normal operation and a much stiffer thermoplastic com-
66 pression spring to absorb the peak loads in storm conditions. This type of
67 mooring tether is combining the two required functions named above, i) suffi-

68 cient compliance during normal sea states and ii) Stiff mooring response in
69 extreme load conditions.

70 *1.2. Brief review on use of rubber moorings*

71 Elastic mooring configurations using rubber materials have been devel-
72 oped for surface and near-surface buoy systems since the mid 60's [9]. The
73 main feature of such elastic, taut buoy systems is the capability to absorb
74 forces induced by the wave action and tidal variations.

75 A direct comparison between elastomeric tethers and a catenary chain
76 configuration carried out by Paul et al. [10] indicates that the former reduce
77 the dynamic tensions in severe sea states by about a third. The use of elastic
78 tethers results in a more moderate buoy motion, increasing the survivability
79 of mooring hardware and instrumentation on the surface buoy [11].

80 As such, one of the most prevalent applications is found in wave buoy
81 moorings [12]. The requirements and applications for wave and navigation
82 buoys are well described in [13]. The mooring system must allow the buoy
83 to track the orbital wave motion, necessitating a highly flexible material.
84 In addition, the elasticity must be relatively constant across the range of
85 extensions. Both aspects are satisfied by rubber, enabling wave buoys to ac-
86 curately measure the wave profile. A specific example are the non-directional
87 Waverider buoys from Datawell, for which a 15m rubber cord (hardness of
88 45 to 50 Shore) is recommended [14].

89 Another application are so-called 'snubbers' [15] which denote rubber
90 inserts in mooring configurations to absorb wave energy. Results from field
91 trials for a buoy based seafloor observation system are reported in [16]. In all
92 three mooring designs the snubber inserts protect the electro-optical cables
93 from undue strains.

94 The use of flexible mooring systems has also been considered for floating
95 marine renewable energy devices. Eight companies that may potentially
96 employ this mooring solution for commercial deployments are identified in
97 [17]. The challenge in incorporating flexible mooring systems to floating
98 marine energy devices is to complement the elastic behaviour in a defined
99 extension range with a non-linear stiff response once the extension exceeds
100 the specified elastic operational limits.

101 A number of systems are proposed to combine these characteristics,
102 among which are the Seaflex buoy mooring system [18] and the Exeter Tether
103 [19, 20]. The preliminary results of a third system, the TFI mooring tether
104 [21] are reported in the remainder of this paper.

105 *1.3. Scope and structure*

106 The key technical consideration for mooring lines is their performance
107 regarding reliability and stiffness characteristics [22]. The testing has been
108 a joint effort of Technology from Ideas (TfI) as technology provider, the
109 wave energy device developer Ocean Power Technologies (OPT) as poten-
110 tial end-user and the University of Exeter who conducted the experiments.
111 The mooring tether combines soft elastomeric and stiff thermoplastic ma-
112 terial components within a single assembly. This allows a soft, elastic re-
113 sponse through the elastomeric component during operational conditions
114 and a stiff, non-linear response through the thermoplastic component to
115 withstand higher loads during storm conditions. Figure 1 shows the design
116 drawing (1(a)) and the assembled prototype (1(b)). The elastomeric part is
117 connected to the centre of two end plates. At the outside of the end plate are
118 two steel wires connected, which are shackled to three compressive elements
119 each. In normal, operating conditions the load response is governed by the

120 elastic component. The steel wires and the compressive elements carry no
121 load in operating conditions. Once the elastomeric element extends to a
122 length where the steel wires are engaged and tensioned, the compressive
123 elements will resist the elongation of tether in a non-linear fashion.

124 The potential of such a combined load response to reduce the peak load-
125 ing of typical mooring arrangements is described in [21]. For the modelled
126 configurations, the maximum tension was reduced up to 90%. The primary
127 purpose of the tests presented in this paper was to confirm the mooring
128 tether could be built to a designed response curve. Industry standard moor-
129 ing packages used by OPT predicted a load reduction by approximately
130 70% for the chosen design curve. Moreover, the mooring tether was experi-
131 mentally tested to assess the load behavior and component performance in
132 different operating conditions.

133 The remainder of the paper describes the experimental set-up and pro-
134 cedure (section 2), followed by the test results of the conducted performance
135 tests (section 3.1), amplitude and frequency hysteresis tests (section 3.2) and
136 the service simulation tests (section 3.3) for the extreme and fatigue load
137 case. The paper closes with a discussion of the main results and outlines
138 the implications for further development (section 4).

139 **2. Experimental set-up and procedures**

140 The objective of the tests were to assess the behaviour and performance
141 of the mooring element and to establish confidence that the required perfor-
142 mance can be delivered in the field. Four specific performance characteristics
143 were assessed:

- 144 1. Load extension response curve of the mooring element

- 145 2. Element operation and performance across a range of sea states
- 146 3. Performance and survival in extreme sea states
- 147 4. Indication of fatigue performance

148 All tests have been carried on the Dynamic Marine Component test rig
149 (DMaC), a unique facility to replicate the forces and motions that com-
150 ponents and sub-systems are subjected to in (floating) marine applications
151 [23–25]. It comprises of two hinged gimbles with a backplate, termed 'mov-
152 ing headstock' which is capable to replicate motions in three degrees of
153 freedom and a linear actuator to provide the axial loading on the specimen.
154 The reaction frame resists the forces and motions induced by the actuators
155 and allows to adjust the linear actuator for a variable test bed length.

156 The experimental set-up of the tether in the rig is shown in fig. 2 and
157 fig. 3. The mooring element was connected to the coupling plate interfaces
158 of the test rig using a series of shackles at both ends, the actuator (fig. 2(b))
159 and the moving headstock (fig. 2(c)). The length of the test bed was
160 adjusted, so that the linear actuator was fully extracted with the mooring
161 element at its original, unstretched, length. Through this set-up a full 1m
162 stroke of the linear actuator was available for the test. The initial length
163 of the unloaded mooring tether (without connectors) is $l_0 = 670mm$, thus
164 a maximum length of $l_{max} = 1670mm$ at a target extension of 149% could
165 be provided by the experimental arrangement.

166

167 Five different test types have been carried out which are briefly described
168 in the following and are summarised in table 1.

- 169 1. *Performance testing*: The load extension curves were measured for
170 slow displacements (10s period) and velocities matching the scaled

171 wave period (3.88s period). The tether was cycled from zero tension
172 at 0m extension to the maximum 1m extension and relaxed again in
173 a smooth manner over a period of 10 seconds. This performance test
174 was repeated throughout the entire test programme to assess potential
175 performance variations. The tether was also cycled from zero tension
176 at 0m extension to a series of target extensions (0.2, 0.4, 0.6 and 0.8m).

177 2. *Hysteresis amplitude testing*: The stress-strain response at non-zero
178 pre-tension levels was measured for a range of different amplitudes.
179 From a zero displacement position the tether was pre-tensioned to
180 target levels of 0.2, 0.3, 0.4 and 0.5m, from which 5 load cycles with
181 amplitudes of 0.1, 0.2 and 0.3m were imposed. The cycle periods were
182 chosen at full-scale periods (8 and 10s) as well as scaled periods (2.4
183 and 3.0s).

184 3. *Hysteresis frequency testing*: This series of tests set out to measure the
185 hysteresis behaviour of the tether for varying wave frequencies/periods.
186 The tether was cycled at two pre-tension levels (0.2 and 0.3m) which
187 are likely to be expected during field operation in a taut mooring
188 system, with a cycle amplitude of 0.1 and 0.2m over a range of wave
189 periods (1.2s to 16s).

190 4. *Extreme sea state/storm condition testing*: In order to be confident
191 in the reliable operation of the tether in extreme sea states, it is es-
192 sential to test the behaviour and integrity in the elastic/thermoplastic
193 transition region of the tether response. The conducted tests included
194 a combination of load cycles replicating a group of five waves, load
195 cycles under high pre-tensions (0.9m) and storm sea conditions using
196 the load signal from a 3-hour numerical simulation.

197 5. *Fatigue testing*: These tests aimed to accelerate the fatigue of the
198 mooring element to deliver confidence that its performance lifetime will
199 be acceptable. The chosen test parameters were based on the expected
200 operational profile with a typical pretension of 0.2m extension and
201 cycle amplitudes of between 2.1s and 3.6s and cycle amplitudes with
202 a peak displacement between 0.23m and 0.62m.

203 The fatigue test were carried out in three blocks, amounting to over
204 1,200 cycles. It is being recognised that the fatigue limit was not being
205 reached during those simulation tests. However an indicative fatigue
206 behaviour could be evaluated.

207 All tests were carried out indoors with room temperatures between 15-20
208 degrees. The test specimen was kept dry, i.e. all tests were conducted in
209 air. It should be noted that all tests were performed on one test specimen.

210 **3. Results**

211 *3.1. Performance tests*

212 The performance test aimed to establish a reference for the tether be-
213 haviour for a full extension. The test was carried out for the individual and
214 coupled elements. The results shown in fig. 4 are plotted for the complete
215 (combined) tether and for the individual elements. This allows identifying
216 the different contributions to the combined tether load response. It can be
217 seen that the load response of the fully assembled tether is initially governed
218 only by the elastic element and with increasing load (extension) the thermo-
219 plastic element engages from about 120% elongation onwards. The results
220 shown have been corrected to exclude the 'rig disturbance' which is caused
221 by stiction forces in the bearings.

Table 1: Test plan summary

Test series	Description	Displacement [m]	Cycle period [s]	Total number of cycles
100	Performance testing	0.2 - 1	3.88, 10	11
200	Hysteresis amplitude testing	0.1 - 0.3	2.4 3.0, 8, 10	93
300	Hysteresis frequency testing	0.3 - 0.5	1.2, 2.1, 3.0, 4, 7, 10, 13, 16	19
400	Extreme/storm testing	0.5 - 1	3.9, 10	18
500-800	Fatigue testing	0.03 - 0.82	2.1, 2.7, 3.0, 3.6, 10	1265

222 The 'modelled' line is a superposition of the individual material stiffness
223 characteristics. The general behaviour is validated through the tests, but
224 the tests reveal two further aspects: i) the mooring tether is slightly softer
225 than expected and that ii) the thermoplastic element shows a considerable
226 hysteresis effect.

227 The hysteresis effect represents the damping provided by the mooring
228 tether, i.e. the energy dissipation E during a single load cycle. This effect
229 can be quantified through numerical integration of the area enclosed by the
230 load-extension curve.

$$E = \int_b^a f(x)dx - \int_b^a g(x)dx \quad (1)$$

231 where $f(x)dx$ is the upper part and $g(x)dx$ the lower part of the load exten-
232 sion curve and the parameters a and b are chosen at the intersections of the

233 curves that enclose the hysteresis area. Using the trapezium rule: $f(x)dx$
234 can be written as:

$$\int_b^a f(x)dx \approx \frac{b-a}{n} \left[\frac{f(a)+f(b)}{2} + \sum_{k=1}^{n-1} f\left(a+k\frac{b-a}{n}\right) \right] \quad (2)$$

235 $g(x)$ is computed in the same manner for values of $g(a)$ and $g(b)$. The
236 amount of damping that is achieved gives an indication how well the peak
237 loads are damped/mitigated by the thermoplastic element and will thus be
238 presented in the following.

239 Figure 5 displays the positive correlation between energy dissipation
240 (hysteresis effect) and increased maximum displacements, i.e. extension of
241 the mooring element.

242 *3.2. Amplitude and frequency hysteresis tests*

243 The aim of the hysteresis amplitude testing was to measure the stress-
244 strain response at non-zero pre-tension levels. The general finding for this
245 test series is that the hysteresis effect depends on the applied pre-tension
246 and cycle amplitude and to a lesser extent on the cycle period.

247 Figure 6 shows the hysteresis values for the three different cycle am-
248 plitudes that have been applied for different pre-tension levels. While an
249 increase of pre-tension for a given cycle amplitude induces a moderate in-
250 crease of the dissipated energy, an increase in the cycle amplitude has a
251 stronger effect.

252 The hysteresis frequency testing aimed to assess the tether behaviour
253 for varying wave frequencies. The relationship between hysteresis effect and
254 cycle period is summarised Fig. 7. For or a given level of pretension and
255 cycle amplitude a slight increase of dissipated energy can be seen up to a
256 period of 5s, which is the frequency relevant at this scale. For higher cycle

257 periods, (7, 10, 13, 16s) the values for the dissipated energy are very similar,
258 which suggests that the elastomer response is not dependent on the incident
259 wave frequency.

260 *3.3. Service simulation tests*

261 *3.3.1. Extreme tests*

262 In order to establish confidence in the reliable operation of the tether
263 in extreme sea states the behaviour and integrity of the tether have been
264 tested in the elastic/thermoplastic transition range. Three different tests
265 were carried out to assess the tether in expected extreme conditions.

- 266 • Simulated wave group with increasing pre-tension and maximum dis-
267 placement that cycles the tether through the elastic/thermoplastic
268 transition.
- 269 • Cyclic test with high pre-tension (0.9m) and ± 0.1 m displacement
- 270 • Storm signal using 100 year storm condition load information

271 Figure 8 shows the simulated wave displacement profile. The five waves
272 peaks and the resulting force are shown where z-axis data denotes the re-
273 quested displacement and 'linear displacement' denotes the measured dis-
274 placement. The simulation achieved good agreement for the displacement
275 signal. It can also be observed (at around 24s) how the thermoplastic ele-
276 ment engages for displacements > 0.8 m and results in a stiffer load response.

277 A more artificial signal aimed to cycle the tether within the elastic-
278 compressive transition region. The recorded load signal is shown in Figure 9.
279 The transition from the elastic to the the thermoplastic element is smooth

280 and repeatable for both increasing and decreasing loads. However, the long-
281 term response, i.e. the fatigue and creep behaviour must also be established
282 (see section 3.3.2).

283 The service simulation appraisal was completed with a load signal de-
284 rived from a 100-year storm model. In order to convert the force signal to
285 a suitable displacement signal, it has been scaled with a factor of $s=3.45$
286 (prototype scale) and normalised with respect to the maximum achievable
287 stroke of 1m. The storm test was run for 45min, equivalent to 3 hours at
288 full-scale. The displacement and force signal for this storm test are shown in
289 Fig 10. The load extension curve largely followed the behaviour established
290 in the earlier tests and the thermoplastic compressive element engaged for
291 some of the peaks demonstrating the working principle of the tether in a
292 realistic load case.

293 3.3.2. *Fatigue tests*

294 The fatigue tests aimed to accelerate the fatigue of the mooring element
295 to gain confidence that its long-term performance will be acceptable. It must
296 be noted here that the scope of the study presented was not sufficient to test
297 the specimens to failure and the number of load cycles have been limited to
298 50 in 4 cases and 500 in one case. The chosen test parameters were based on
299 the expected operational profile with a typical pretension of 0.2m extension
300 and cycle amplitudes of between 2.1s and 3.6s and cycle amplitudes with a
301 peak displacement between 0.23m and 0.62m (see Table 2). The most severe
302 profile was also tested with $N = 500$ cycles.

303 The nominal energy dissipation for each cycle is shown in Figure 11
304 and reveals a slight decrease throughout the test, that appears to stabilise
305 around 5.7% reduction compared to the first load cycle. The fatigue tests

Table 2: Fatigue tests

Test No.	Pretension [m]	Relaxation [m]	Peak Displacement [m]	Cycle period [s]	Number of cycles
510	0.2	0.01	0.23	2.1	50
530	0.2	0.03	0.29	2.7	50
550	0.2	0.06	0.38	3	50
570	0.2	0.14	0.62	3.6	50
805	0.2	0.14	0.62	3.6	500

Table 3: Percentage loss of hysteresis effect for different fatigue tests

N	Test number				
	510	530	550	570	805
50	-5.5%	-5.4%	-4.1%	-3.7%	-7.2%
500					-5.7%

306 only exercise the elastic element, so the loss of hysteresis is attributed to
307 the relaxation/creep of the tether.

308 3.4. Creep Analysis

309 As with all polymer materials there will be some permanent creep de-
310 formation to the materials over repeated stress/strain events [26, 27]. The
311 mooring element consists of two separate polymer components, the rubber
312 elastomer and the thermoplastic spring, each with separate creep perfor-
313 mance. By plotting the peak force achieved at a defined extension, this creep
314 can be measured in order to estimate the creep for the expected component
315 lifetime. Figure 12(a) shows the results of such a plot on the elastomeric
316 component alone extended by 0.8m. The green dots represent actual mea-

317 surements with the red line being the curve fitted to those dots. It can
318 be seen that there are inconsistencies where the force drops by substan-
319 tial amounts over a single extension. These can be traced to experimental
320 changes, where the mooring element has been disassembled or changed in
321 some way between tests. Removing these inconsistencies we obtain the green
322 line.

323 Figure 12(b) shows the same analysis over the entire component
324 stretched to 1m extension. In this case there are some larger inconsistencies
325 which can be traced to a design issue with the connectors which has emerged
326 through the tests but can be easily mitigated. Once these points are removed
327 a value for the expected creep can be obtained. These results show that the
328 there is a reduction in the peak load at 1m extension of approximately 14%
329 over 10 million cycles. This can be further reduced by preconditioning the
330 component, stretching it at the manufacturing stage before deployment to
331 remove the initial creep, halving the peak load loss at 1m extension. Due to
332 the non-linear nature of the stress/strain response curve, the mooring com-
333 ponent only requires an additional 1% extension of the mooring component
334 to reach the original peak load, resulting in creep having very little impact
335 on performance.

336 **4. Discussion and Conclusion**

337 This paper has presented some of the key results for a performance and
338 service simulation test of a novel mooring tether. The working principle
339 has been successfully demonstrated in that the elastomeric elastic element
340 is engaged in normal operating conditions and the thermoplastic compres-
341 sive element engages for in situations of high/extreme mooring loads. This

342 allows a mooring system with both a 'soft' response to allow the motion of
343 the floating device necessary for many power take-off designs and a 'stiff'
344 response for high load situations, for example during storms. A prototype
345 of this mooring tether was tested for this work, but the main response char-
346 acteristics and the point of transition from the elastic to the compressive
347 element can be designed for the application at hand. The fatigue and creep
348 analysis work has also indicated the lifetime expectations for such compo-
349 nents, suggesting 5-10 year lifetimes are feasible.

350 The presented behaviour will be very useful for array configuration of
351 devices where the footprint area must be tightly controlled to avoid inter-
352 ference or collision of closely spaced devices [21]. It also overcomes the
353 dilemma that mooring cost is directly coupled to the expected peak load
354 during storm conditions and the required maximum breaking load of the
355 mooring material, as two systems are combined to decouple operational and
356 extreme mooring requirements.

357 Further tests will have to be conducted to investigate the frequency de-
358 pendence of the tether under submerged conditions, which are expected to
359 differ from the conditions in air. Beyond the initial assessment presented
360 here, further tests must also validate the fatigue performance in a test-to-
361 failure approach for multiple specimen.

362 The performance and service simulation tests identified a number of
363 small design changes to be made to the mooring component. Following
364 successful tank testing of the components it is planned to deploy tethers
365 rated to 50kN on a full sized data buoy in Galway Bay, Ireland during 2014.

366 **Acknowledgements**

367 The authors would like to acknowledge the support of the lead author
368 through the UK Centre for Marine Energy Research (UKCMER) under
369 the SuperGen marine programme funded by the Engineering and Physical
370 Sciences Research Council (EPSRC), grant EP/I027912/1 ([www.supergen-](http://www.supergen-marine.org.uk)
371 [marine.org.uk](http://www.supergen-marine.org.uk)). The development of the component test rig was made possi-
372 ble through funding by the Peninsula Research Institute for Marine Renew-
373 able Energy (PRIMaRE), which was supported by the European Regional
374 Development fund (ERDF) and the former South West Regional Develop-
375 ment Agency (SWRDA). Acknowledgement is also made to Dr. Andrew
376 Vickers who supported the test work.

- 377 [1] BVG Associates, Wave and tidal energy in the pentland firth and orkney
378 waters: How the projects could be built., Tech. rep., The Crown Estate,
379 a report commissioned by The Crown Estate and prepared by BVG
380 Associates (2011).
- 381 [2] W. M. J. J. P. S. Butterfield, Charles P., L. Wayman, Engineering
382 challenges for floating offshore wind turbines, in: Offshore Wind Con-
383 ference, National Renewable Energy Laboratory (NREL), Copenhagen,
384 Denmark, 2007.
- 385 [3] S.-P. Breton, G. Moe, Status, plans and technologies for offshore wind
386 turbines in Europe and North America, *Renewable Energy* 34 (3) (2009)
387 646 – 654.
- 388 [4] L. Johanning, G. H. Smith, J. Wolfram, Towards design standards for
389 WEC moorings, in: Proc. European Wave and Tidal Energy Conference
390 (EWTEC), Glasgow, 2005.
- 391 [5] L. Johanning, G. H. Smith, J. Wolfram, Mooring design approach for
392 wave energy converters, Proceedings of the Institution of Mechanical
393 Engineers, Part M: Journal of Engineering for the Maritime Environ-
394 ment 220 (4) (2006) 159–174. doi:10.1243/14750902JEME54.
- 395 [6] L. Johanning, G. H. Smith, J. Wolfram, Measurements of static
396 and dynamic mooring line damping and their importance for float-
397 ing WEC devices, *Ocean Engineering* 34 (1415) (2007) 1918 – 1934.
398 doi:10.1016/j.oceaneng.2007.04.002.
- 399 [7] G. Dalton, R. Alcorn, T. Lewis, A 10 year installation pro-
400 gram for wave energy in Ireland: A case study sensitivity analy-

- 401 sis on financial returns, *Renewable Energy* 40 (1) (2012) 80 – 89.
402 doi:10.1016/j.renene.2011.09.025.
- 403 [8] L. Johannig, G. H. Smith, Consideration of the cost implications for
404 mooring mec devices, Deliverable D7.3.2 Grant Nr. 213380, Equitable
405 Testing and Evaluation of Marine Energy Extraction Devices in terms of
406 Performance, Cost and Environmental Impact EQUIMAR (July 2009).
- 407 [9] D. Wyman, Elastic tethering techniques for surface and near-surface
408 buoy systems, in: *Proc. of OCEANS '82*, 1982, pp. 610–613.
409 doi:10.1109/OCEANS.1982.1151849.
- 410 [10] W. Paul, J. Irish, J. Gobat, M. Grosenbaugh, Coastal mooring de-
411 sign: taut elastomeric and chain catenary surface buoy moorings, in:
412 *OCEANS '99 MTS/IEEE. Riding the Crest into the 21st Century*, Vol.
413 Vol. 1, 1999. doi:10.1109/OCEANS.1999.799781.
- 414 [11] W. Paul, J. Irish, Providing electrical power in conjunction with elas-
415 tomeric buoy moorings, in: *Proc. of Ocean Community Conference 98*,
416 Marine Technology Society, 1998, pp. 928–932.
- 417 [12] J. Wood, J. Irish, A compliant surface mooring system for real time
418 data acquisition, in: *Proc. of OCEANS '87*, 1987, pp. 652–657.
- 419 [13] H. P. Joosten, R. Scrivens, Elastic mooring of wave and navigation
420 buoys, International Ocean Systems, 2006.
- 421 [14] B. Datawell, Datawell waverider reference manual (2006).
- 422 [15] J. L. Brown, In-line snubber for use with braided cordage, uS Patent
423 4,258,608 (Mar. 31 1981).

- 424 [16] W. Paul, M. Chaffey, A. Hamilton, S. Boduch, The use of
425 snubbers as strain limiters in ocean moorings, in: OCEANS,
426 2005. Proceedings of MTS/IEEE, 2005, pp. 2722–2729 Vol. 3.
427 doi:10.1109/OCEANS.2005.1640185.
- 428 [17] A. Bowie, Flexible moorings for tidal current turbines, Master’s thesis,
429 University of Strathclyde. Department of Mechanical and Aerospace
430 Engineering. (2012).
- 431 [18] N. Bengtsson, V. Ekström, Increase life cycle and decrease cost for
432 navigation buoys, Tech. rep., Seaflex Buoy mooring system (2010).
433 URL <http://buoymooring.com/data/archive/White-Paper-SEAFLEX-Buoy-Mooring.pdf>
- 434 [19] L. Johannig, D. Parish, Mooring limb, uS Patent App. 13/522,504
435 (Jan. 18 2011).
- 436 [20] L. Johannig, University of Exeter – Testing novel mooring compo-
437 nents, Presentation, superGen UK Centre for Marine Energy Research
438 Annual Assembly 2013 (2013).
- 439 [21] P. McEvoy, Combined elastomeric and thermoplastic mooring tethers,
440 in: Proc. of 4th Int. Conf. on Ocean Energy, Dublin, Ireland, 2012.
- 441 [22] R. Harris, L. Johannig, J. Wolfram, Mooring systems for wave energy
442 converters: A review of design issues and choices, in: Proc. of 3rd Int.
443 Conference on Marine Renewable Energy (MAREC), Blyth, UK, 2004.
- 444 [23] P. R. Thies, L. Johannig, G. H. Smith, Towards component reliability
445 testing for marine energy converters, Ocean Engineering 38 (2-3) (2011)
446 360 – 370. doi:10.1016/j.oceaneng.2010.11.011.

447 [24] P. R. Thies, L. Johanning, T. Gordelier, A. Vickers, S. Weller, Physi-
448 cal component testing to simulate dynamic marine load conditions, in:
449 Proc. of 32nd Int. Conference on Ocean, Offshore and Arctic Engineer-
450 ing (OMAE), no. OMAE2013-10820, Nantes, France,, 2013.

451 [25] P. R. Thies, L. Johanning, T. Gordelier, Component reliability testing
452 for wave energy converters: Rationale and implementation, in: Proc. of
453 10th European Wave and Tidal Energy Conference EWTEC, Aalborg,
454 Denmark, 2013.

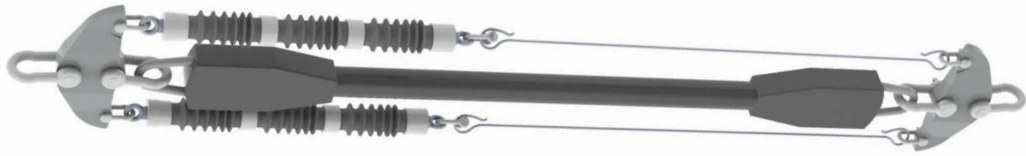
455 [26] I. M. Ward, D. Hadley, An introduction to the mechanical properties
456 of solid polymers, no. ISBN: 0-471-93874-2, Wiley & Sons, 1993.

457 [27] F. Khan, C. Yeakle, Experimental investigation and modeling of non-
458 monotonic creep behavior in polymers, International Journal of Plas-
459 ticity 27 (4) (2011) 512 – 521. doi:10.1016/j.ijplas.2010.06.007.

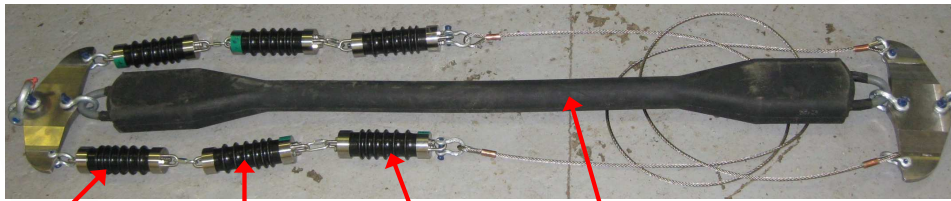
460 **List of Figures**

461	1	Prototype Tfl mooring tether combining elastomeric and	
462		thermoplastic elements.	25
463	2	Experimental set-up of mooring element in Dynamic Marine	
464		component test rig (DMaC)	26
465	3	Test set-up for individual components	27

466	4	Load-extension performance of individual tether components	
467		(elastomeric and thermoplastic characteristics) and combined	
468		tether performance (corrected for test rig disturbance). Test	
469		rig disturbance has been quantified through a test run with-	
470		out specimen attached. The anticipated modelled behaviour	
471		(solid curve) is also shown.	27
472	5	Energy dissipation (hysteresis effect) for increased maximum	
473		displacements of the mooring element	28
474	6	Pretension against Hysteresis for Test 200 series	29
475	7	Cycle period against Hysteresis for Test 300 series	30
476	8	Displacement signal and recorded linear force for simulated	
477		wave group test. Thermoplastic element engaged at peak	
478		around 24s.	31
479	9	Repeated cycling over elastic-compressive transition.	32
480	10	100 year storm condition test, close-up view	33
481	11	Number of cycles and hysteretic behaviour during fatigue tests	34
482	12	Analysis of measured and expected creep performance of	
483		mooring tether	35



(a) Design drawing for mooring tether

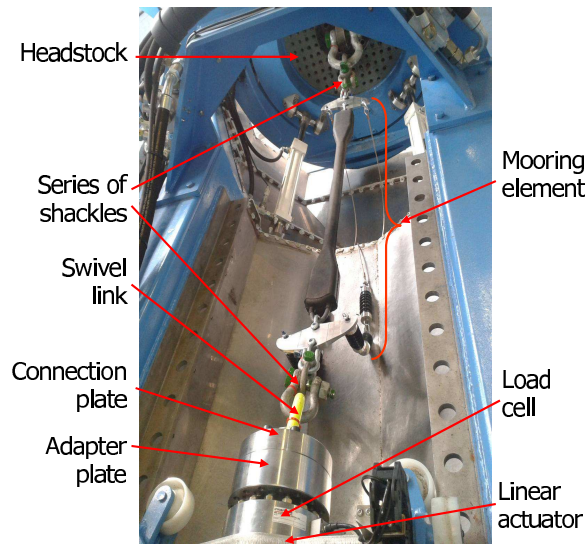


Thermoplastic compressive elements

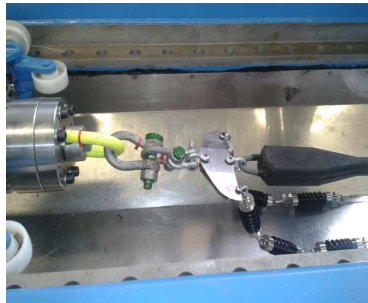
Elastomeric elastic element

(b) Assembled prototype

Figure 1: Prototype Tfl mooring tether combining elastomeric and thermoplastic elements.



(a) Overview from linear actuator

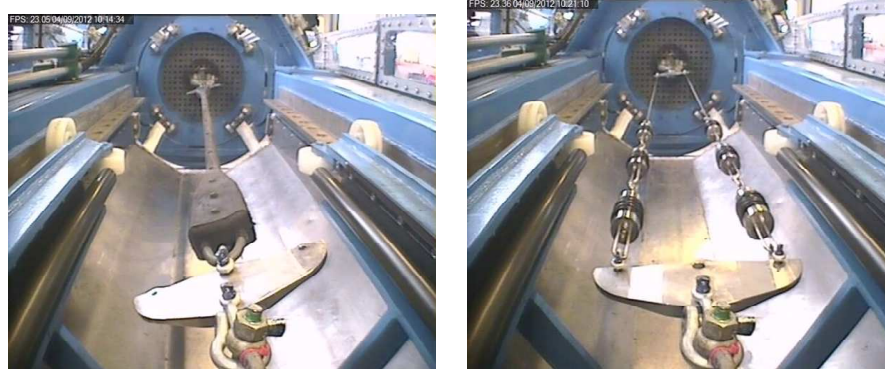


(b) Connection to linear actuator



(c) Connection to headstock

Figure 2: Experimental set-up of mooring element in Dynamic Marine component test rig (DMaC)



(a) Elastomeric elastic component (b) Thermoplastic compressive element

Figure 3: Test set-up for individual components

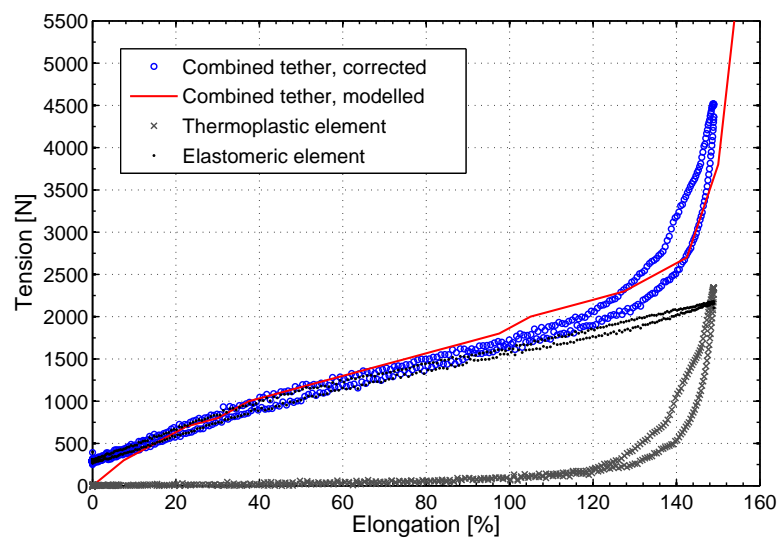


Figure 4: Load-extension performance of individual tether components (elastomeric and thermoplastic characteristics) and combined tether performance (corrected for test rig disturbance). Test rig disturbance has been quantified through a test run without specimen attached. The anticipated modelled behaviour (solid curve) is also shown.

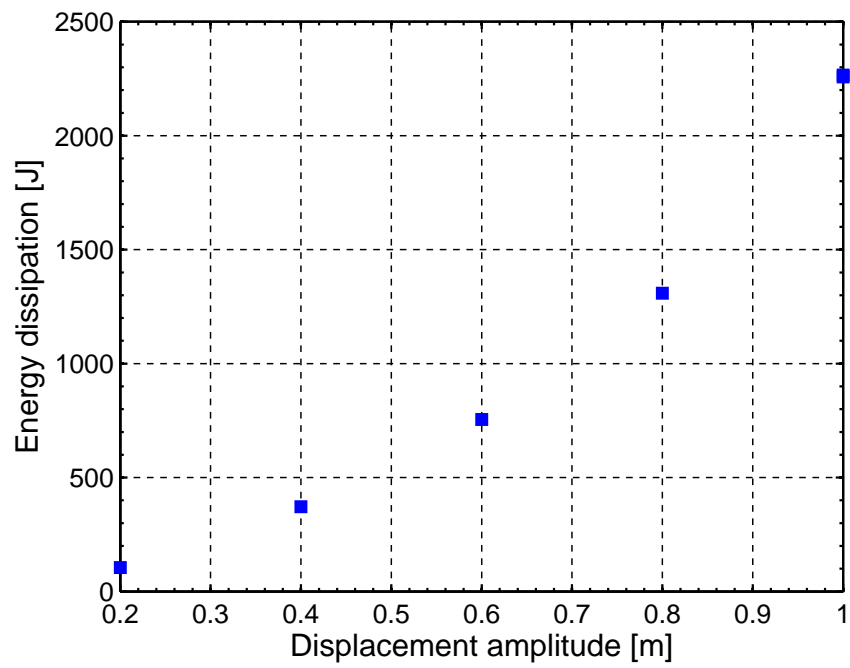


Figure 5: Energy dissipation (hysteresis effect) for increased maximum displacements of the mooring element

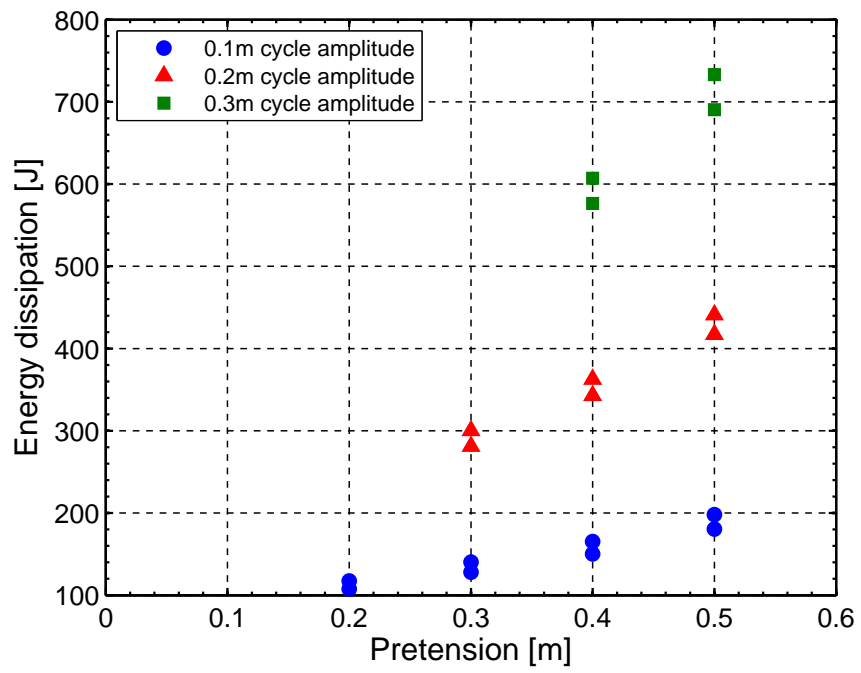


Figure 6: Pretension against Hysteresis for Test 200 series

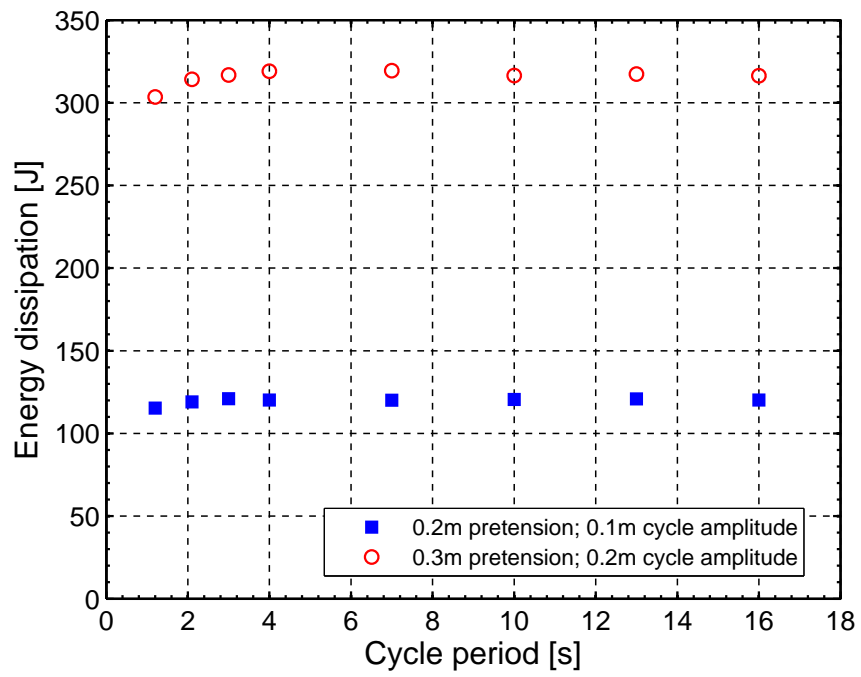


Figure 7: Cycle period against Hysteresis for Test 300 series

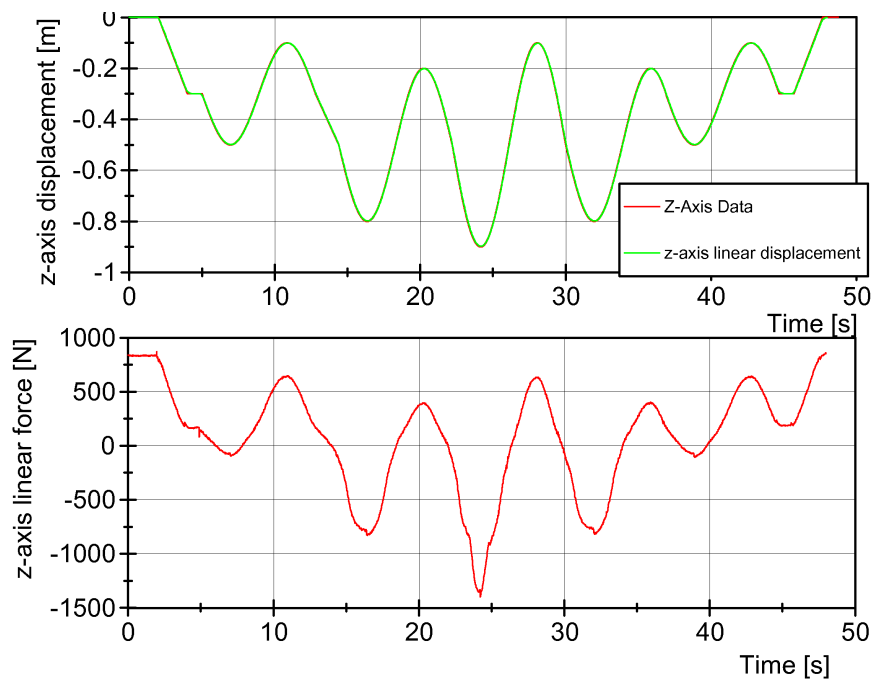


Figure 8: Displacement signal and recorded linear force for simulated wave group test. Thermoplastic element engaged at peak around 24s.

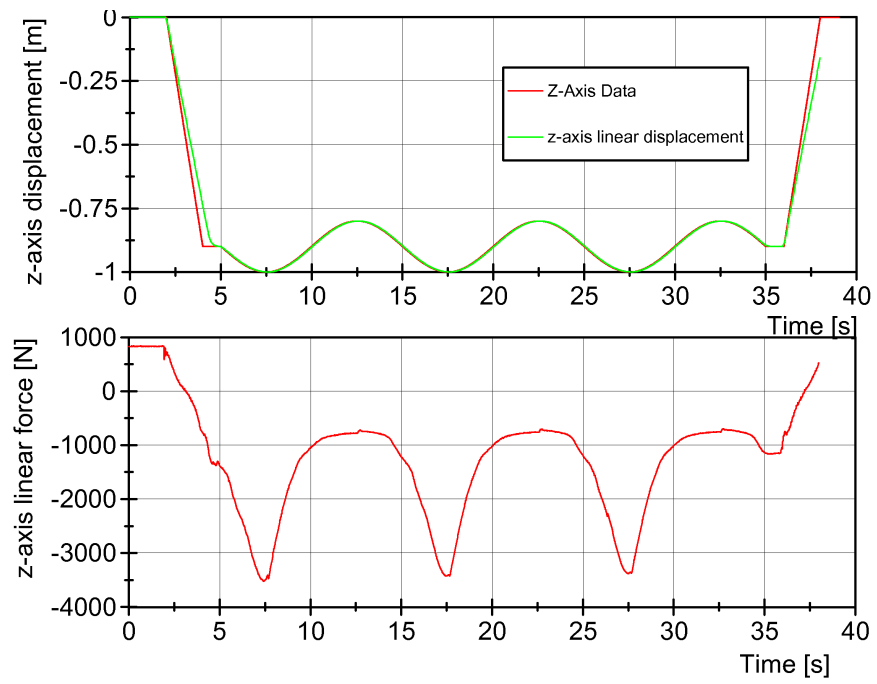


Figure 9: Repeated cycling over elastic-compressive transition.

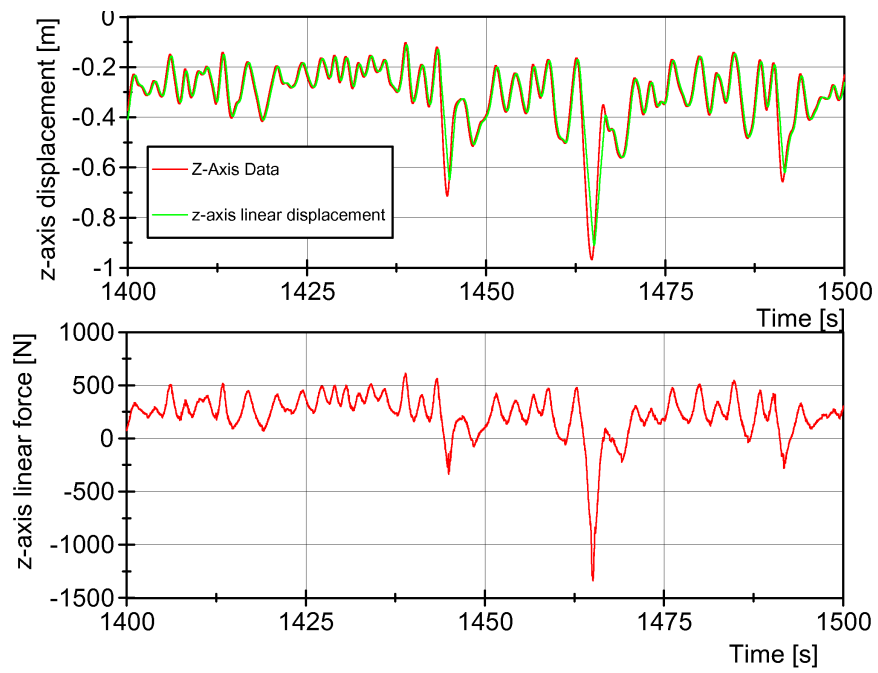


Figure 10: 100 year storm condition test, close-up view

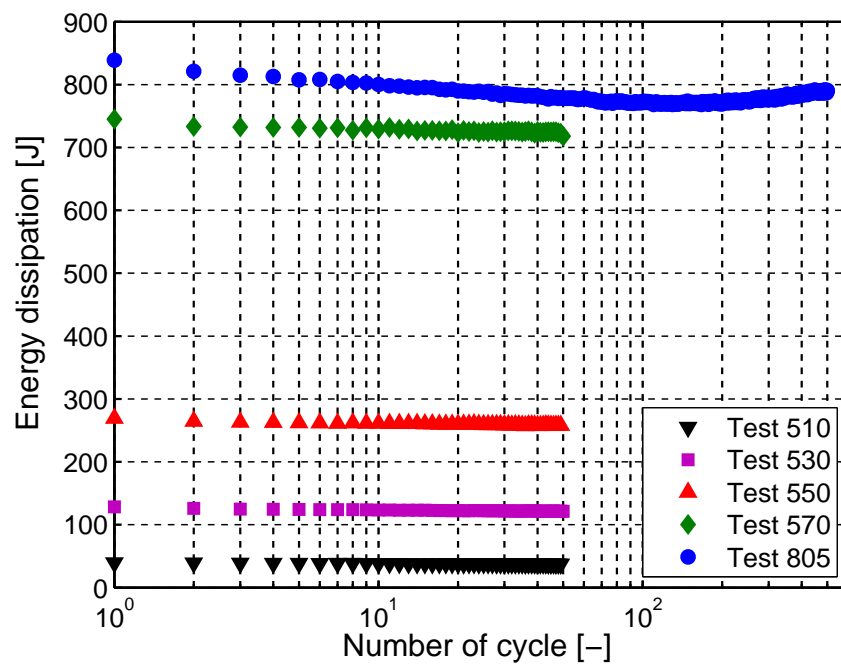
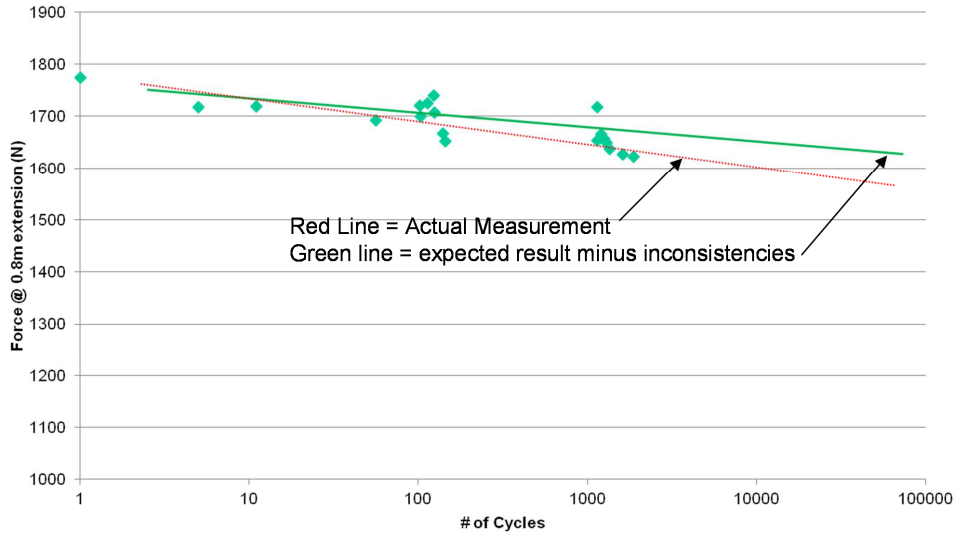
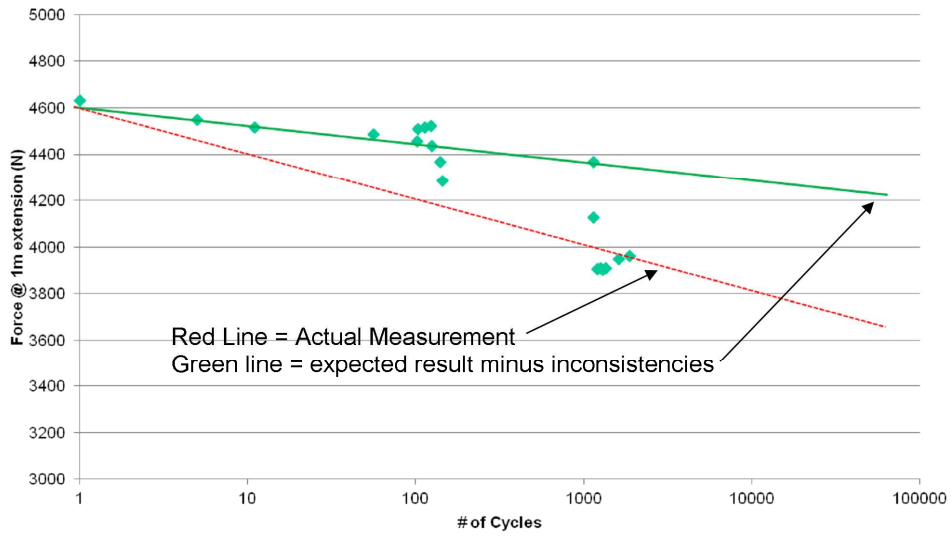


Figure 11: Number of cycles and hysteretic behaviour during fatigue tests



(a) Elastomer, 0.8m extension



(b) Entire tether, 1.0m extension

Figure 12: Analysis of measured and expected creep performance of mooring tether